DOI: 10.1002/ejic.201100424

Propellers and Planes: Phosphorescent Pt^{II} σ-Acetylides from Polyaromatic Ligands

Deanne Nolan,[a] Belén Gil,[a] Frances A. Murphy,[a] and Sylvia M. Draper*[a]

Keywords: Platinum / Isomers / Alkyne ligands / Graphene / Photophysics

This article details the preparation, photophysical and electrochemical investigation of four novel polyaromatic square-planar platinum(II) bis(acetylide) complexes, incorporating either a planar hexa-*peri*-hexabenzocoronene (**L²**) or its uncyclised ethynyl-hexaphenylbenzene precursor (**L¹**). Complexes in both *cis* and *trans* geometries (*cis*-[Pt(**L**)$_2$(dppe)] [**C¹**, **C²**; dppe = 1,2-bis(diphenylphosphanyl)ethane] and *trans*-[Pt(**L**)$_2$(PPh$_3$)$_2$] (**T¹**, **T²**) were successfully prepared and fully characterised. The low-energy bands of the UV/Vis absorption spectra for the uncyclised family (**L¹**, **C¹**, **T¹**) and for the cyclised family (**L²**, **C²**, **T²**) exhibit a redshift in the order *trans* > *cis* > ligand, indicating enhanced π-conjugation along the molecular axis in *trans* configuration. Each Pt^{II} complex is dual luminescent and possesses a high-energy ligand-centred fluorescence and a lower energy emission with significant phosphorescent character facilitated by the high spin-orbit coupling of the heavy platinum metal centre. Notably, *cis*- and *trans*-**L²** complexes exhibit remarkably long lifetimes in degassed CH_2Cl_2 at room temperature (*trans*: 30.9 μs; *cis*: 18.3 μs) for sharp phosphorescence at λ = 578 nm.

Introduction

Hexa-*peri*-hexabenzocoronenes (HBCs) offer a unique polyaromatic motif for application in molecular electronic devices. They demonstrate a desirable set of physical, electronic and structural properties arising primarily from their highly delocalised π-electrons and their ability to aggregate via columnar π-π stacking.[1] Their propeller-like polyphenylene precursors have also attracted attention in dendrimer research and as supramolecular hosts to a variety of guest molecules.[2]

Given the scarcity of organometallic HBC derivatives[3,4] and the well-documented improvement in the phosphorescence quantum yields of π-conjugated organic materials on incorporating heavy metal centres,[5–7] this article details the preparation, photophysical and electrochemical investigation of two new polyaromatic ligands and their Pt^{II} σ-acetylide complexes. The work builds on just three known compounds that couple one HBC platform to a Pt^{II} metal centre.[3] These exhibit enhanced singlet-triplet mixing due to the spin-orbit coupling of the metal centre and a propensity to aggregate in solution and the solid-state. The increased steric bulk and additional geometric complexity of attaching two HBC platforms to one Pt^{II} centre was a synthetic challenge, which might enable a more in-depth study of aspects of the chemistry of HBC-related complexes.

Despite the thermodynamic stability of *trans*-Pt^{II} bis(acetylides), the *cis*-configured complexes were generated by using a chelating auxiliary phosphane.[8] This provided a means by which to systematically compare both *cis* and *trans* structural isomers for the first time.[9]

Results and Discussion

Synthesis and Characterisation

Four square-planar platinum(II) bis(acetylide) complexes were prepared, two with *cis* and two with *trans* conformation. Iodo-hexaphenylbenzene (I-HBC) was the key synthon in the preparation of both ligands **L¹** and **L²** (Scheme 1).[10] Sonogashira cross-coupling between I-HBC and (trimethylsilyl)acetylene by using *cis*-$PdCl_2(PPh_3)_2$ as catalyst and CuI as co-catalyst gave the protected precursor, which on subsequent deprotection by using KF resulted in **L¹** in 90.5% yield (see Experimental Section).

Sonogashira–Hagihara coupling reactions were used to prepare *cis*-[Pt(**L¹**)$_2$(dppe)] (**C¹**) and *cis*-[Pt(**L²**)$_2$(dppe)] (**C²**) and *trans*-[Pt(**L¹**)$_2$(PPh$_3$)$_2$] (**T¹**) and *trans*-[Pt(**L²**)$_2$(PPh$_3$)$_2$] (**T²**) (Scheme 1).[11] *cis*-[PtCl$_2$(dppe)] incorporating bidentate 1,2-bis(diphenylphosphanyl)ethane (dppe) was used to generate the *cis* complexes.[12] Those in *trans* configuration could be prepared by using *cis*-[PtCl$_2$(PPh$_3$)$_2$][13] due the relative thermodynamic stability of the *trans* configuration.

The four complexes were characterised by NMR spectroscopy (^{1}H, ^{13}C{^{1}H}, ^{31}P{^{1}H}), IR spectroscopy, mass spectrometry and elemental analysis. ^{31}P{^{1}H} NMR spectroscopy proved a useful tool in confirming the *cis*/*trans* configuration. For *trans* complexes, the single upfield

[a] School of Chemistry, University of Dublin, Trinity College Dublin 2, Ireland
Fax: +353-1-671-2826
E-mail: smdraper@tcd.ie

Supporting information for this article is available on the WWW under http://dx.doi.org/10.1002/ejic.201100424.

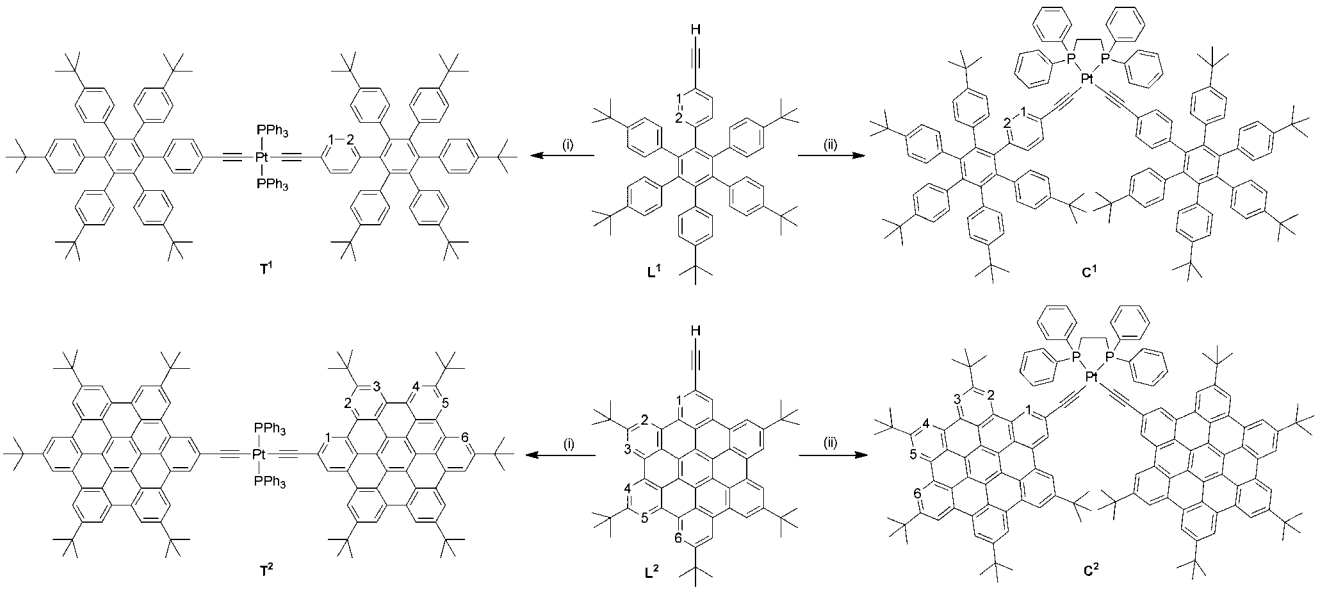

Scheme 1. Synthesis of *cis* and *trans* complexes **T¹**, **T²**, **C¹**, **C²**. Key: (i) *cis*-[$Pt(PPh_3)_2Cl_2$] (0.5 equiv.), CuI (cat.), CH_2Cl_2/*i*Pr_2NH; (ii) *cis*-[Pt(dppe)Cl_2] (0.5 equiv.), CuI (cat.), CH_2Cl_2/*i*Pr_2NH.

Table 1. Selected spectroscopic data for complexes **T¹**, **T²**, **C¹** and **C²**.

Complex	$^{31}P\{^1H\}$:[a] δ [ppm] ($J_{P,Pt}$ [Hz])	$^{13}C\{^1H\}$[b] (C≡C): δ [ppm]	IR:[c] $\tilde{\nu}$(C≡C) [cm^{-1}]
T¹	19.31 (2657)	116.4, 114.1	2110
T²	18.96 (2625)	115.4, 113.7	2093
C¹	41.26 (2279)	113.0, 112.8	2106, 2118 (sh)
C²	41.22 (2279)	113.6, 112.8	2104, 2109

[a] $^{31}P\{^1H\}$ NMR ($CDCl_3$, room temp., 162 MHz). [b] $^{13}C\{^1H\}$ NMR ($CDCl_3$, room temp.), 100 MHz (**T²**), 151 MHz (**T¹**, **C¹**, **C²**). [c] Neat solid-state samples.

$^{31}P\{^1H\}$ signal appears with its platinum satellites having typically large *trans* coupling constants. The larger *trans* influence of the C≡C group relative to the phosphane ligand mean that the *trans* $^{31}P\{^1H\}$ signals are upfield compared to those of the corresponding *cis* isomers (Table 1).

The ^1H NMR spectra of **L¹** and **L²** were also simplified by the C_2 axis within each molecule. The phenyl protons on uncyclised **L¹** occur as a series of overlapping AB signals between δ = 6.6 and 7.0 ppm. The aromatic region of the ^1H NMR spectrum of HBC **L²** consists of 6 singlets appearing between δ = 8.6 and 9.2 ppm. The aromatic proton closest to the acetylene group (H^1) is the most shielded of these (see Scheme 1 for ^1H NMR labelling).[8]

For the complexes, H^1 and H^2 give the most upfield-shifted aromatic signals. In **T¹**, the H^1 signal is shifted significantly upfield at δ = 5.80 ppm, compared to δ = 6.58 ppm in **C¹** due to the difference in the *trans* influence of the phosphane and acetylide ligands. The same is true for **C²** and **T²**, i.e. the H^1 in **T²** is more shielded (**T²**: δ = 8.42 ppm; **C²**: δ = 9.22 ppm). Neither spectra showed concentration dependence in the range 10^{-3} to 10^{-6} M.

For each complex, two signals due to quaternary carbon atoms are observed in the $^{13}C\{^1H\}$ NMR spectra that correspond to C^{α}≡C^{β} of the acetylide. Unfortunately, despite long accumulation times, it was not possible to extract coupling constants and thereby distinguish C^{α} from C^{β}.

IR spectroscopy confirmed the coordination geometry of the complexes. There were two C≡C bands for the C_{2v} (*cis*) complexes and just one for the D_{2h} (*trans*) complexes (Table 1). The molecular weights of the four complexes were verified by MALDI-TOF mass spectrometry and their purity established by elemental analysis.

X-ray Crystallography

Single crystals of iodo-hexaphenylbenzene (I-HBC), a key synthon for **L¹** and **L²** (Scheme 1), suitable for X-ray diffraction were grown by slow concentration of a CH_2Cl_2/CH_3OH solution of the compound. The molecule crystallises in the $P2_1/c$ space group with one molecule of I-HBC and two molecules of CH_2Cl_2 in the asymmetric unit. The molecule has a propeller-like structure, with the six phenyl substituents twisted at angles between 66 and 71° from the plane of the central benzene ring.

The iodine atoms are involved in an interaction (3.611 Å) with a C–C bond on the adjacent *tert*-butylphenyl group of a second molecule of I-HBC (Figure 1). This interaction causes the formation of a dimeric pair; CH_2Cl_2 solvent molecules play a key role in the packing. They form an unusual interaction between their protons and the phenyl rings of iodo-hexaphenylbenzene (shorter than the sum of the

van der Waals radii for H and C atoms, 2.623–2.716 Å). Subsequent batches of crystals obtained from CH_2Cl_2/CH_3OH solvent mixtures gave the identical crystal structure with the same CH_2Cl_2–phenyl interactions.

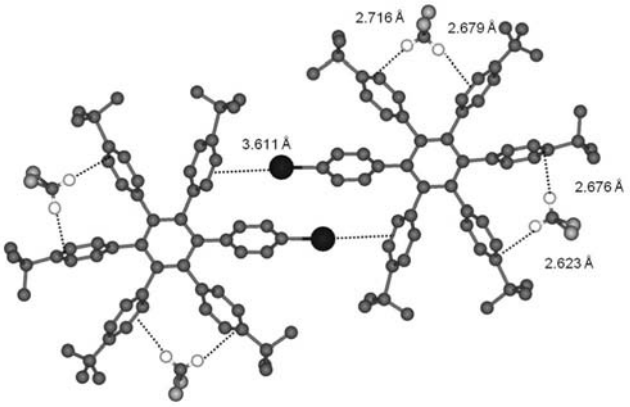

Figure 1. Ball-and-stick representation of two molecules of iodohexaphenylbenzene (I-HBC) showing the intermolecular interactions and the role of the CH_2Cl_2 solvent molecules in the crystal structure (H atoms omitted from I-HBC for clarity).

Dimeric pairs of molecules are arranged in linear arrays, which can be considered as sheets of molecules (Figure 2). Adjacent sheets are offset from each other, and the overall supramolecular structure is reminiscent of a bilayer in biological structures. The iodo-phenyl head groups face each other at the interior interface, and the polyphenyl substituents form the outer surfaces.

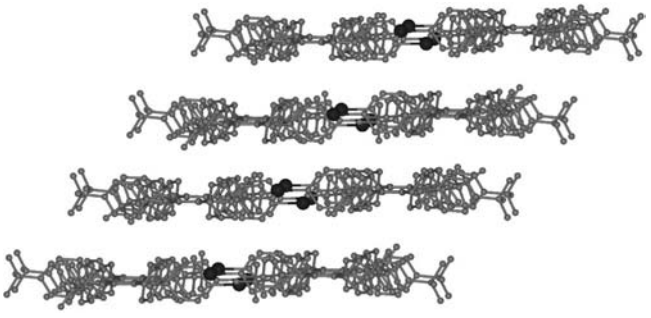

Figure 2. Packing of molecules in the crystal structure of I-HBC showing the formation of dimeric pairs of molecules in sheet-like layers.

UV/Vis Absorption Spectroscopy

The absorption spectrum of ligand **L¹** is broad and featureless and typical of a non-planar polyphenylene (Figure 3).[15] The main bands are π-π* in origin and are centred in the near-UV region (λ_{max} = 257 nm, Table S1). In contrast, the increased planarity and rigidity of cyclised **L²** results in the well-resolved bands and significant fine structure characteristic of hexa-*peri*-hexabenzocoronenes (Figure 4).[10,16]

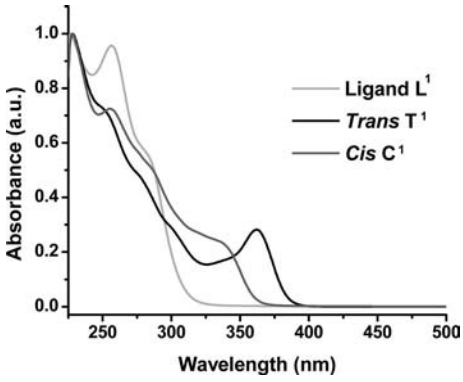

Figure 3. Normalised UV/Vis absorption spectra of **L¹**, **C¹** and **T¹** in CH_2Cl_2 (ca. 10^{-5} M).

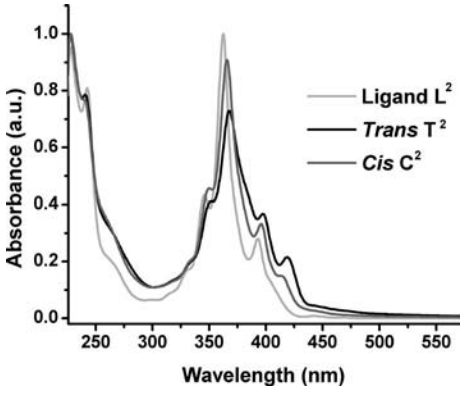

Figure 4. Normalised UV/Vis absorption spectra of **L²**, **C²** and **T²** in CH_2Cl_2 (ca. 10^{-5} M).

The *cis* and *trans* uncyclised complexes **C¹** and **T¹** also exhibit intense ligand-based absorption bands in the near-UV region (Figure 3) and in addition a redshifted MLCT band that occurs at longer wavelengths for **T¹** than for **C¹** due to more effective electronic communication through the Pt^{II} centre in the *trans* configuration (**C¹**: 337 nm; **T¹**: 362 nm).[8b,9,17] Absorption spectra for cyclised complexes **C²** and **T²** are dominated by typical HBC bands but again show slight redshifts on moving from ligand to *cis* to *trans* complex[10] (β-band at 363 nm for **L²**, 365 nm for **C²**, and 367 nm for **T²**; Figure 4).

The extra absorption observed for **C²** and **T²** (**C²**: 414 nm; **T²**: 419 nm) compared to **L²** may be a result of some intraligand character with a contribution from an MLCT transition. The appearance of this additional band has been attributed to the fact that the attachment of a Pt–acetylide group breaks the symmetry of the HBC.[3b] It has also been observed in a recently reported terpyridyl-substituted HBC.[10]

Electrochemical Properties

Cyclic voltammetric (CV) studies were carried out on 1 mM solutions of the ligands and complexes in CH_2Cl_2

(0.1 M nBu_4NPF_6). The results are summarised in Table 2. Poor solubility of **T²** at suitable concentrations precluded CV measurement in this case.

Table 2. Electrochemical data for ligands **L¹**, **L²** and complexes **C¹**, **T¹** and **C²**.[a]

Compound	Oxidation $E_{1/2}$ [V]	Reduction $E_{1/2}$ [V][d]
L¹	–[b]	–1.93
C¹	0.66,[c] 0.96	–1.92
T¹	0.60,[c] 0.99	–1.90
L²	0.57, 0.83	–1.96
C²	0.49,[c] 0.87	–1.93
Pt(HBC)[6b]	0.8[c]	–

[a] In dichloromethane (0.1 M, nBu_4NPF_6) at 298 K, scan rate = 100 mVs^{-1}, reported vs. Fc/Fc^+. [b] No oxidation process observed within 0.0–2.0 V spectral window. [c] Irreversible/quasireversible oxidation process, E_{pa} [V] (anodic peak potential) quoted. [d] Return oxidation wave associated with this reduction poorly defined.

The redox behaviour of polyphenylene ligand **L¹** is significantly different to that observed for HBC ligand **L²**; **L¹** displays no oxidation process within the solvent window (+0.0 to +2.0 V), whereas two reversible oxidations are evident for **L²**, with $E_{1/2}$ = +0.57 and +0.83 V (Figure S1) as is common for HBC derivatives.[18] The two reversible oxidation peaks seen in **L²** are also seen in complex **C²**. However, in **C²** the irreversible Pt^{II}/Pt^{III} oxidation is coincident with the first oxidation on the ligand, and so this oxidation peak appears as a broadened signal on the CV (Figure S1). A reversible reduction is observed between –1.9 and –2.0 V for both ligands and complexes; however, the associated reverse oxidation process appears as a relatively broad peak, implying a degree of quasireversibility.

Photoluminescence Spectroscopy

Table 3 summarises selected photoluminescence data for uncyclised **L¹** and its corresponding *cis* and *trans* complexes **C¹** and **T¹** in argon-degassed CH_2Cl_2 solution and in the solid-state at 298 and 77 K, including lifetimes (at 298 K) and quantum yields.

In degassed CH_2Cl_2 (10^{-5} M) solution (Figure 5), emission from **L¹**, **C¹** and **T¹** is dependent on the excitation wavelength. Excitation at high energies ($\lambda \approx 280$ nm) induces strong emission, whereas a less intense redshifted band is observed upon excitation at lower energy. For the complexes, this lower energy emission is significantly more structured than the higher energy band. In **T¹** it shows a vibronic progression of ca. 2200 cm^{-1} consistent with the involvement of the C≡C unit in the electronic transition. Lifetimes for each of these emission bands are in the nanosecond region and slightly enhanced on moving from ligand to complex.

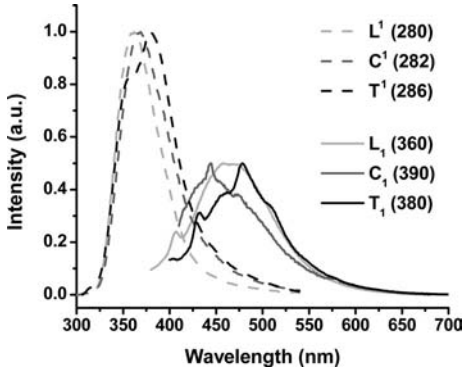

Figure 5. Normalised emission spectra showing the two emission bands (excitation wavelength dependent) of **L¹**, **C¹** and **T¹** in argon-degassed CH_2Cl_2 at 298 K (λ_{exc} [nm]).

In the solid state, the emission of **L¹** is similar to that in solution appearing at room temperature as a broad band (λ_{max} = 354 nm) with an extended tail (Figure S2). Excitation of uncyclised *cis* (**C¹**) and *trans* (**T¹**) complexes at 315 nm results in significantly more redshifted emission bands (**C¹**: λ_{max} = 377 nm; **T¹**: λ_{max} = 372 nm) and slight lifetime enhancement on going from **L¹** (36.0, 7.9 ns) to **C¹**

Table 3. Emission data for uncyclised ligand **L¹** and its *cis* (**C¹**) and *trans* (**T¹**) complexes.

	Medium (T [K])	λ_{em} [nm] (λ_{exc} [nm])	τ [ns]	Φ_{em}[a]
L¹	solid (298)	354 (305)	36.0 (88%), 7.9 (12%) (λ_{exc} 295 – λ_{em} 355)	
	solid (77)	350_{max}, 455, 488 (305)		
	CH_2Cl_2 (298)[b]	362 (280), 465 (360)	18.7 (61%), 5.5 (39%) (λ_{exc} 295 – λ_{em} 370) 6.6 (73%), 14.9 (27%) (λ_{exc} 370 – λ_{em} 460)	< 0.001
	CH_2Cl_2 (77)	345_{max}, 447, 479 (285)		
C¹	solid (298)	377_{max}, 482, 513_{sh} (315)	39.9 (89%), 14.9 (11%) (λ_{exc} 295 – λ_{em} 375) 1.1×10^3 (80%), 0.2×10^3 (20%) (λ_{exc} 370 – λ_{em} 480)	
	solid (77)	481_{max}, 540 (350)		
	CH_2Cl_2 (298)[b]	368 (282), 375_{sh}, 395 (350) 444, 465_{sh} (390)	20.3 (56%), 7.2 (44%) (λ_{exc} 295 – λ_{em} 370) 23.1 (67%), 7.1 (33%) (λ_{exc} 370 – λ_{em} 460)	0.022
	CH_2Cl_2 (77)	467_{max}, 494, 516_{sh} (330)		
T¹	solid (298)	372_{max}, 386, 481, 518 (315)	51.0 (44%), 30.6 (56%) (λ_{exc} 295 – λ_{em} 375) 4.4×10^3 (74%), 0.6×10^3 (26%) (λ_{exc} 370 – λ_{em} 480)	
	solid (77)	477_{max}, 521 (360)		
	CH_2Cl_2 (298)[b]	355_{sh}, 374_{max} (286), 433, 458, 478_{max}, 508_{sh}(380)	24.1 (69%), 7.1 (31%) (λ_{exc} 295 – λ_{em} 370) 39.4 (38%), 8.4 (62%) (λ_{exc} 370 – λ_{em} 460)	0.005
	CH_2Cl_2 (77)	471_{max}, 512 (365)		

[a] Measured by using quinine sulfate as a standard. [b] Argon-degassed solution, ca. 10^{-5} M.

(39.9, 14.9 ns) to **T¹** (51.0, 30.6 ns). This is consistent with the Pt^{II} centre affecting the polyphenylene emission by causing an extension of π-conjugation along the molecular axis.

As observed in solution, **C¹** and **T¹** exhibit an additional broad lower energy emission band in the solid-state (**C¹**: 482 nm; **T¹**: 481 nm) with significantly enhanced lifetimes (**C¹**: 1.1, 0.2 μs; **T¹**: 4.4, 0.6 μs) due to phosphorescence facilitated by the high spin-orbit coupling of the metal centre. In contrast, for both **C¹** and **T¹** at 77 K in the solid-state (Figure 6) and in frozen CH_2Cl_2 (Figure S3), only a lower energy phosphorescence is evident (CH_2Cl_2: **C¹**: λ_{max} = 467 nm; **T¹**: λ_{max} = 471 nm; solid: **C¹**: λ_{max} = 481 nm; **T¹**: λ_{max} = 477 nm), attributable to a $^3\pi$-π^* transition with some Pt^{II} influence.

Table 4 summarises selected photoluminescence data for HBC **L²** and its corresponding *cis* and *trans* complexes **C²** and **T²** in argon-degassed CH_2Cl_2 solution and in the solid-state at 298 and 77 K, including lifetimes (at 298 K) and quantum yields. The CH_2Cl_2 data was concentration-independent (10^{-5} to 10^{-12} M), and no aggregation dependence was observed for complexes **C²** and **T²**.

In the solid state at room temperature, emission from cyclised HBC ligand **L²** appears as a broad quite structured band with λ_{max} = 509 nm (Figure 7). An almost identical luminescence profile is observed for the *cis* (**C²**) and *trans* (**T²**) complexes; however, as observed for the uncyclised family, lifetimes ($\lambda_{em} \approx 505$ nm) are enhanced from ligand to complex enabled by the attached metal centre and again from *cis* to *trans* complex due to more efficient electronic

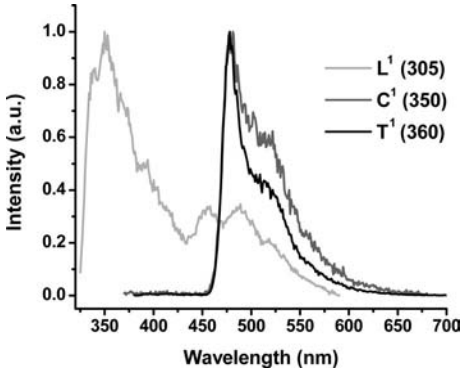

Figure 6. Normalised emission spectra of **L¹**, **C¹** and **T¹** in the solid-state at 77 K (λ_{exc} [nm]).

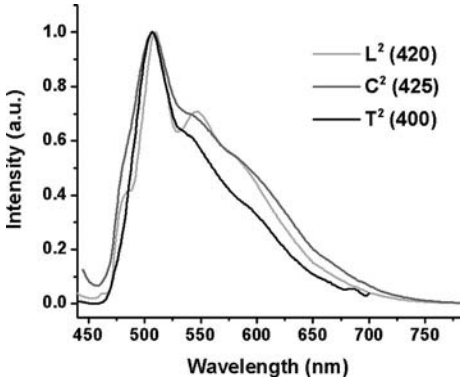

Figure 7. Normalised emission spectra of **L²**, **C²** and **T²** in the solid-state at 298 K (λ_{exc} [nm]).

Table 4. Emission data for cyclised ligand **L²** and its *cis* (**C²**) and *trans* (**T²**) complexes.

	Medium (*T* [K])	λ_{em} [nm] (λ_{exc} [nm])	τ [ns]	Φ_{em}[a]
L²	solid (298)	483, 509_{max}, 546, 580_{sh} (420)	1.1×10^3 (81%), 0.2×10^3 (19%) (λ_{exc} 370 – λ_{em} 508)	
	solid (77)	483, 512_{max}, 546, 581_{sh} (420)		
	CH_2Cl_2 (298)[b]	460_{wk}, 471_{max}, 481, 490, 500, 524, 535, 545_{sh}, 563_{wk} (335)	12.1 (3%), 24.2 (97%) (λ_{exc} 370 – λ_{em} 470) 18.1 (68%), 6.3 (32%) (λ_{exc} 460 – λ_{em} 500)	0.093
	CH_2Cl_2 (298)[c]	460_{wk}, 471_{max}, 481, 491, 500, 525, 535, 545_{sh}, 565_{wk} (390)		0.079
	CH_2Cl_2 (77)	463_{sh}, 475_{max}, 486, 497, 506, 534, 544, 579, 636_{wk} (420)		
C²	solid (298)	482_{sh}, 508_{max}, 542_{sh}, 590_{sh} (425)	4.8×10^3 (74%), 0.6×10^3 (26%) (λ_{exc} 370 – λ_{em} 510)	
	solid (77)	512, 577_{max}, 625, 657_{wk} (425)		
	CH_2Cl_2 (298)[b]	473, 481, 492, 502, 526, 536_{wk}, 577_{max}, 625, 656_{wk} (420)	19.2 (85%), 6.4 (15%) (λ_{exc} 370 – λ_{em} 470) 18.3×10^3 (100%) (λ_{exc} 370 – λ_{em} 578)	0.021
	CH_2Cl_2 (298)[c]	453_{wk}, 473, 483, 493_{max}, 502, 515_{sh}, 527, 538, 548_{sh}, 567_{wk}, 575_{wk}, 616_{sh} (405)		0.095
	CH_2Cl_2 (77)	471_{wk}, 481_{wk}, 491_{wk}, 500_{wk}, 526_{wk}, 573_{max}, 582_{sh}, 621, 631, 653_{wk} (400)		
T²	solid (298)	506_{max}, 540, 591_{sh} (400)	12.4×10^3 (79%), 1.1×10^3 (21%) (λ_{exc} 370 – λ_{em} 505)	
	solid (77)	506, 542_{sh}, 577_{max}, 625, 633_{wk} (420)		
	CH_2Cl_2 (298)[b]	471, 481, 491, 501, 525_{wk}, 536_{wk}, 578_{max}, 626, 636_{sh}, 657_{wk} (405)	23.2 (85%), 13.6 (15%) (λ_{exc} 370 – λ_{em} 472) 30.9×10^3 (100%) (λ_{exc} 370 – λ_{em} 578)	0.018
	CH_2Cl_2 (298)[c]	473, 482, 493, 503_{max}, 527, 536, 577_{wk} (408)		0.032
	CH_2Cl_2 (77)	491_{wk}, 574_{max}, 623, 633_{sh}, 654_{wk} (420)		

[a] Measured by using 4′,6-diamidino-2-phenylindole dihydrochloride as a standard. [b] Argon-degassed solution, ca. 10^{-5} M. [c] Oxygenated solution, ca. 10^{-5} M.

delocalisation ($\mathbf{L^2}$: 1.1, 0.2 μs; $\mathbf{C^2}$: 4.8, 0.6 μs; $\mathbf{T^2}$: 12.4, 1.1 μs).

The emissions of $\mathbf{C^2}$ and $\mathbf{T^2}$ change at lower temperatures. At 298 K a broad and unstructured HBC-based emission can be identified for both complexes, but the spectra at 77 K (Figure 8) are dominated by an intense very-narrow-band-width emission at λ = 577 nm with an additional vibronic band at 625 nm. This is assigned to phosphorescence from the HBC chromophore facilitated by the attached platinum(II) acetylide.[3b]

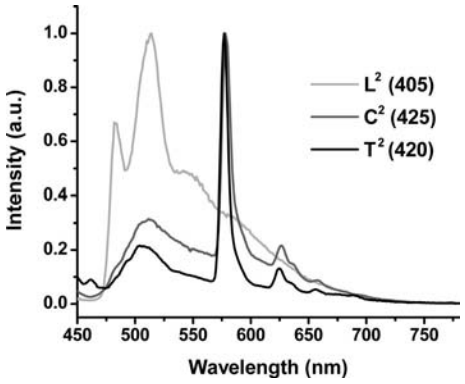

Figure 8. Normalised emission spectra of $\mathbf{L^2}$, $\mathbf{C^2}$ and $\mathbf{T^2}$ in the solid-state at 77 K (λ_{exc} [nm]).

In Ar-degassed CH_2Cl_2 solution, narrow-band-width phosphorescence from the HBC chromophore is again the dominant feature ($\mathbf{C^2}$: λ_{max} = 577 nm; $\mathbf{T^2}$: λ_{max} = 578 nm; Figure 9). The onset of typical HBC fluorescence occurs at 470 nm (mimicking that observed for $\mathbf{L^2}$), and the lifetimes recorded for ligand and complexes at this emission maximum are comparable (ca. 20 ns, ca. 10 ns). The ratio of phosphorescence/HBC fluorescence is large in both cases ($\mathbf{C^2}$: 5:1; $\mathbf{T^2}$: 20:1), with the *trans* complex ($\mathbf{T^2}$) experiencing the effect of the attached metal centre considerably more than the *cis* complex ($\mathbf{C^2}$). The recorded lifetimes for the phosphorescent band (λ = 578 nm) of both $\mathbf{C^2}$ and $\mathbf{T^2}$ are remarkably long (λ_{exc} = 370 nm: $\mathbf{T^2}$: 30.9 μs; $\mathbf{C^2}$: 18.3 μs). Such very long lifetimes correspond to the assignment of this emission as being derived from a triplet excited state located on the HBC chromophore.[6b] The marked difference in triplet lifetime observed between *trans* ($\mathbf{T^2}$) and *cis* ($\mathbf{C^2}$) complex is a further indicator that π-conjugation is most efficient when the acetylide ligands are coordinated *trans*.[10]

HBC-derived phosphorescence is highly oxygen-sensitive (Figure 10). In oxygenated CH_2Cl_2 solutions, only the vibronic fine structure of fluorescence from the HBC platform is evident for both $\mathbf{C^2}$ and $\mathbf{T^2}$, with solely residual fluorescence from the ligand evident at 578 nm. The opposite effect is observed for both complexes at 77 K in frozen CH_2Cl_2 (Figure S2) – the intensity of HBC fluorescence drops further relative to phosphorescence, which is blue-shifted slightly for both complexes ($\mathbf{C^2}$: λ_{max} = 573 nm; $\mathbf{T^2}$: λ_{max} = 574 nm). Specifically, the ratio of phosphorescence/fluorescence increases to 25:1 for $\mathbf{C^2}$ and 131:1 for $\mathbf{T^2}$.

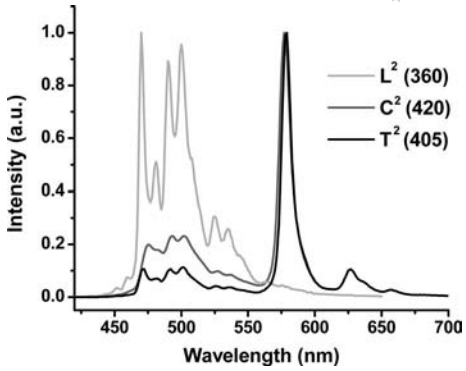

Figure 9. Normalised emission spectra of $\mathbf{L^2}$, $\mathbf{C^2}$ and $\mathbf{T^2}$ in argon-degassed CH_2Cl_2 (ca. 10^{-5} M) at 298 K (λ_{exc} [nm]).

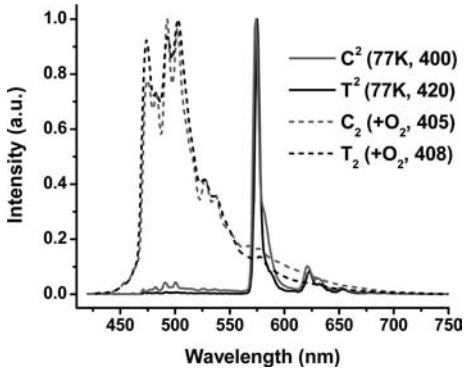

Figure 10. Normalised emission spectra of $\mathbf{C^2}$ and $\mathbf{T^2}$ in CH_2Cl_2 at 77 K and in oxygenated solution at 298 K (ca. 10^{-5} M) (conditions, λ_{exc} [nm]).

It has been previously reported that the lifetime of the triplet state is reduced as a result of aggregation, an effect that would have been anticipated for HBC complexes $\mathbf{C^2}$ and $\mathbf{T^2}$.[3b] However, no aggregation was observed for these complexes under photophysical examination or by NMR spectroscopy. We suggest that the effect of the *tert*-butyl groups along the periphery of the HBC and the presence of the bulky phosphanes in the complexes prevents such stacking. Despite the potential for the twisting of the aromatic ligand platforms about the Pt–σ-acetylide bonds no concentration effects were observed.

Conclusions

This work details the synthesis of four novel Pt^{II} σ-acetylide molecular systems incorporating uncyclised propeller ligand $\mathbf{L^1}$ and its corresponding fully cyclised HBC $\mathbf{L^2}$. Complexes in both *cis* and *trans* geometries were successfully prepared by careful choice of the platinum(II) precursor by using either a monodentate or a bidentate phosphanyl auxiliary ligand. All the complexes were fully characterised by spectroscopic and analytical methods.

The optical properties of uncyclised $\mathbf{L^1}$ and planarised ligand $\mathbf{L^2}$ are very different. Highly structured redshifted bands in the UV/Vis and emission spectra of $\mathbf{L^2}$ occur as a result of enhanced π-electron delocalisation within the mo-

lecule and its enforced planarity. In non-planar polyphenylene **L¹**, no effective conjugation between the rings means that such features are entirely absent with instead quite broad and featureless optical spectra recorded; **L²** displays notably longer emission lifetimes in both solution and in the solid-state and improved quantum yields as is characteristic of hexa-*peri*-hexabenzocoronenes.[19]

Both uncyclised and cyclised sets of Pt^{II} compounds are dual-luminescent. They each possess a higher energy ligand-based fluorescence, slightly redshifted and with longer lifetimes than the corresponding free ligand. In both cyclised and uncyclised compounds, strong spin-orbit coupling induced by the heavy metal Pt^{II} centre stabilises the triplet excited state on the acetylide.[8b] As a result, the lower energy bands have significant phosphorescent character, as evidenced by the longer lifetimes recorded. HBC complexes **C²** and **T²** exhibit remarkably long lifetimes for the sharp phosphorescent band at 578 nm in degassed CH_2Cl_2 (**T²**: 30.9 μs; **C²**: 18.3 μs). Moving from *cis* to *trans* complexes, less positive Pt^{II}/Pt^{III} oxidation potentials, slightly enhanced fluorescence lifetimes, redshifted absorption bands in the UV spectra and notably extended phosphorescence lifetimes are observed. In combination, these results clearly demonstrate that the *trans* arrangement of acetylide ligands on the Pt^{II} centre is optimal for π-conjugation along the molecular axis.

Experimental Section

General Methods: Unless otherwise stated, all reactions were carried out under nitrogen or argon with dry solvent, freshly distilled under anhydrous conditions. Starting materials (trimethylsilyl)-acetylene, KF, CuI and $MgSO_4$ (Sigma–Aldrich) and K_2PtCl_4 (Alfa–Aesar) and standard solvents were used without further purification. The known compounds 2-ethynyl-5,8,11,14,17-penta-*tert*-butylhexa-*peri*-hexabenzocoronene (**L²**) and 1-(4-iodophenyl)-2,3,4,5,6-penta-*tert*-butylphenylbenzene (**1**),[10] $PdCl_2(PPh_3)_3$,[20] *cis*-$[PtCl_2(PPh_3)_2]$[13] and *cis*-$[Pt(dppe)Cl_2]$[12] were synthesised according to literature procedures. NMR spectra were recorded in $CDCl_3$ with (i) Bruker Avance DPX-400 spectrometer (operating at 400.1 MHz for ^1H, 100.6 MHz for ^{13}C), (ii) Bruker AV-600 spectrometer (600.1 MHz for ^1H, 150.6 MHz for ^{13}C), (iii) Bruker AV-400 spectrometer (162 MHz for ^{31}P). ^1H and ^{13}C NMR spectra were referenced relative to TMS (δ = 0.00 ppm) and ^{31}P NMR spectra relative to H_3PO_4 as an external standard. ^{13}C and ^{31}P NMR spectra were proton-decoupled. Chemical shifts (δ) are reported in ppm and coupling contants in Hz. For the NMR characterisation of the complexes, *i*, *o*, *m* and *p* refer to the *ipso*, *ortho*, *meta* and *para* carbon atoms, respectively, on the phosphane moiety; pt = pseudo-triplet and pd = pseudo-doublet. IR spectra (reported in cm^{-1}) of neat samples were recorded with a Perkin–Elmer Spectrum-One FT-IR spectrometer equipped with a Universal-ATR sampling accessory. Electrospray mass spectra were recorded with a Micromass-LCT spectrometer, and accurate mass spectra were referenced against leucine enkephalin (555.6 $g\,mol^{-1}$) and reported to within 5 ppm. MALDI-TOF mass spectra were recorded with a Waters MALDI-QTOF Premier spectrometer by using an α-cyano-4-hydroxycinnamic acid matrix, and accurate mass spectra were referenced against [Glu¹]-Fibrinopeptide B (1570.6 $g\,mol^{-1}$) and reported to within 5 ppm. Elemental analyses were performed in the Microanalytical Laboratory, University College Dublin.

Electrochemical Measurements: Cyclic voltammetry was performed by using a CH Instruments Electrochemical Analyser Model 600B. Cyclic voltammograms were measured on 1 mM solutions of ligands and complexes in CH_2Cl_2 by using tetra-*n*-butylammonium hexafluorophosphate ($TBAPF_6$, 0.1 M) as supporting electrolyte. A standard three-electrode cell was employed with a glassy carbon working electrode, a Pt wire counter electrode, and an SCE as the reference electrode. Potentials are quoted vs. the ferrocene/ferrocenium couple (0.0 V), and all potentials were referenced to internal ferrocene added at the end of each experiment. Solutions were degassed for several minutes by nitrogen bubbling before the experiments were performed, and a flow of nitrogen over the solution was maintained for the duration of the experiment.

Photophysical Measurements: UV/Vis absorption spectra were recorded as optically dilute solutions (10^{-4} to 5×10^{-7} M) in 1×1 cm^2 quartz cuvettes with a Shimadzu UV-2450 spectrophotometer. Corrected steady-state solution (ca. 10^{-5} M) and solid-state emission spectra at 298 and 77 K were recorded with a Horiba–Jobin–Yvon Fluorolog 3-22 spectrometer with double grating emission and excitation monochromators. A Jobin–Yvon FluoroHub single-photon counting controller fitted with a 295 or a 370 nm Jobin–Yvon NanoLED was used to measure lifetimes, which were determined from the observed decays by using DataStation v2.4. Emission quantum yields of the solutions were measured by the Demas and Crosby[21] method and were measured relative to quinine sulfate in 0.5 M H_2SO_4 (Φ_{em} = 0.546),[22] or relative to 4′,6-diamidino-2-phenylindole dihydrochloride (DAPI) in water (Φ_{em} = 0.042).[23] Corrections were made for the difference in refractive index of the sample and reference solutions.

Crystal Structure Determination: A suitable crystal of 1-(4-iodophenyl)-2,3,4,5,6-penta-(4-*tert*-butylphenyl)benzene (**1**) with size of $0.40\times0.20\times0.20$ mm was selected, covered with inert oil and mounted on a quartz fibre tip and immediately placed on the goniometer head in a 150 K N_2 stream. The structure converged to a reasonable *R* factor. Further details are provided in the Supporting Information. CCDC-783244 contains the supplementary crystallographic data for this paper. These data can be obtained free of charge from The Cambridge Crystallographic Data Centre via www.ccdc.cam.ac.uk/data_request/cif.

1-(4-Ethynylphenyl)-2,3,4,5,6-penta-(4-*tert*-butylphenyl)benzene (L¹): 1-(4-Iodophenyl)-2,3,4,5,6-penta-(4-*tert*-butylphenyl)benzene (**1**; 731.4 mg, 0.777 mmol) was dissolved in dry, distilled THF (90 mL) and *i*Pr_2NH (30 mL). The solution was degassed (freeze-pump-thaw cycles). (Trimethylsilyl)acetylene (0.33 mL, 2.331 mmol), *cis*-$PdCl_2(PPh_3)_2$ (32.9 mg, 6 mol-%), and CuI (9.3 mg, 6 mol-%) were added, and the reaction was stirred under nitrogen at room temperature over 3 d. After this time, the solvent was removed, CH_2Cl_2 (ca. 5 mL) was added to the residue to form a suspension, and this was then added to a stirring excess of methanol (ca. 100 mL). The product 1,2,3,4,5-pentakis(4-*tert*-butylphenyl)-6-{4-[(trimethylsilyl)ethynyl]phenyl}benzene was obtained by filtration as an off-white powder (665.1 mg, 94.0%). This product (665.1 mg, 0.730 mmol) was redissolved in a mixture of THF/CH_2Cl_2 (150 mL:100 mL). KF (412.0 mg, 7.091 mmol) in excess methanol (150 mL) was added to the reaction mixture, which was then stirred at room temperature under nitrogen overnight. The solvent was removed in vacuo, and the residue was dissolved in excess CH_2Cl_2 (ca. 300 mL) and washed with water (3×200 mL). The organic layer was reduced in volume (ca. 5 mL), and the product was obtained as an off-white powder by filtration after precipitation with excess methanol (ca. 150 mL) (554.0 mg, 90.5%).

1,2,3,4,5-Pentakis(4-*tert*-butylphenyl)-6-{4-[(trimethylsilyl)ethynyl]-phenyl}benzene: ^1H NMR (600 MHz, $CDCl_3$, 25 °C, atom labelling

as for **L¹** in Scheme 1): δ = 6.98 [d, ^3J(H,H) = 8.0 Hz, 2 H, H^1], 6.77–6.83 (m, 12 H, H^2, H_{phenyl}), 6.61–6.68 (m, 10 H, H_{phenyl}), 1.12 [s, 18 H, C(CH_3)$_3$], 1.09 [s, 27 H, C(CH_3)$_3$], 0.18 [s, 9 H, Si(CH_3)$_3$] ppm. $^{13}C\{^1H\}$ NMR (100.6 MHz, $CDCl_3$, 25 °C): δ = 147.9 (C_{quat}), 147.6 (C_{quat}), 147.5 (C_{quat}), 142.0 (C_{quat}), 140.9 (C_{quat}), 140.2 (C_{quat}), 139.0 (C_{quat}), 137.9 (C_{quat}), 137.7 (C_{quat}), 135.6 (C_{quat}), 133.7 (C_{quat}), 131.7 (1 C, *C*H, C^2), 131.2 (*C*H), 131.1 (2 C, *C*H), 130.4 (1 C, *C*H, C^1), 123.5 (*C*H), 123.2 (*C*H), 123.1 (*C*H), 119.3 (*C*H), 106.0 (1 C, C_{quat}, C≡C), 93.1 (1 C, C_{quat}, C≡C), 34.3 [2 C, C_{quat}, *C*(CH$_3$)$_3$], 34.2 [3 C, C_{quat}, *C*(CH$_3$)$_3$], 31.3 [15 C, C(*C*H$_3$)$_3$], 0.1 [3 C, Si(*C*H$_3$)$_3$] ppm. ES-MS (THF): calcd. for $[C_{67}H_{78}NaSi]^+$ 933.5771; found 933.5785 $[M + Na]^+$.

L¹: M.p. > 200 °C (decomp.). ^1H NMR (400.2 MHz, $CDCl_3$, 25 °C, atom labelling as for **L¹** in Scheme 1): δ = 6.99 [d, ^3J(H,H) = 8.5 Hz, 2 H, H^1], 6.78–6.84 (m, 12 H, H^2, H_{phenyl}), 6.62–6.68 (m, 10 H, H_{phenyl}), 2.92 (s, 1 H, C≡C*H*), 1.12 [s, 18 H, C(CH_3)$_3$], 1.09 [s, 27 H, C(CH_3)$_3$] ppm. $^{13}C\{^1H\}$ NMR (100.6 MHz, $CDCl_3$, 25 °C): δ = 147.8 (C_{quat}), 147.5 (C_{quat}), 147.4 (C_{quat}), 142.2 (C_{quat}), 140.9 (C_{quat}), 140.7 (C_{quat}), 140.0 (C_{quat}), 138.9 (C_{quat}), 137.8 (C_{quat}), 137.7 (C_{quat}), 137.5 (C_{quat}), 131.6 (1 C, *C*H, C^2), 131.1 (*C*H), 131.0 (*C*H), 130.3 (1 C, *C*H, C^1), 123.4 (*C*H), 123.1 (*C*H), 123.1 (*C*H), 118.2 (C_{quat}), 84.4 (1 C, C_{quat}, *C*≡CH), 77.2 (1 C, C≡*C*H), 34.1 [2 C, C_{quat}, *C*(CH$_3$)$_3$], 34.0 [3 C, C_{quat}, *C*(CH$_3$)$_3$], 31.2 [s, 15 C, C(*C*H$_3$)$_3$] ppm. ES-MS (THF): calcd. for $[C_{64}H_{70}Na]^+$ 861.5375; found 861.5387 $[M + Na]^+$. $C_{64}H_{70}$ (839.25): calcd. C 91.59, H 8.41; found C 91.72, H 8.29.

General Synthetic Procedure for C¹, C², T¹, T²: A solution of CH_2Cl_2/*i*Pr_2NH was degassed by freeze-pump-thaw cycles and transferred to a dry Schlenk flask containing the appropriate platinum(II) chloride precursor, polyaromatic acetylene and CuI as catalyst. The solution was stirred in the dark at room temperature over several days. When the reaction was complete, the solvent was removed in vacuo and the residue redissolved in CH_2Cl_2/$CHCl_3$ and washed with water (3×). The organic layer was dried with $MgSO_4$ and the solvent removed to dryness. **C¹**, **T¹** and **T²** were purified by column chromatography on silica and precipitation by addition of methanol. **C²** was obtained as a pure solid by precipitation from methanol without the need for column chromatography. Atom labelling for NMR assignments as for **L¹** and **L²** in Scheme 1.

***trans*-[Pt(L¹)$_2$(PPh$_3$)$_2$] (T¹): T¹** was prepared according to the general synthetic procedure by using **L¹** (100.3 mg, 0.120 mmol), *cis*-$PtCl_2(PPh_3)_2$ (46.6 mg, 0.059 mmol), and CuI (0.8 mg, 7 mol-%) in still-dried CH_2Cl_2/*i*Pr_2NH (ca. 5:1, v/v; 20 mL:4 mL) under argon for 36 h. Following washing, column chromatography on silica was performed by eluting with hexane/CH_2Cl_2 (2:1, v/v). Precipitation yielded the product as an off-white powder (80.0 mg, 56.6%). M.p. > 280 °C (decomp.). ^1H NMR (600 MHz, $CDCl_3$, 25 °C): δ = 7.68 (m, 12 H, H^o), 7.24 [t, ^3J(H,H) = 7.3 Hz, 6 H, H^p], 7.17 [t, ^3J(H,H) = 7.3 Hz, 12 H, H^m], 6.83 [d, ^3J(H,H) = 8.2 Hz, 8 H, H^3], 6.81 (m, 4 H, H^7), 6.79 [d, ^3J(H,H) = 8.2 Hz, 8 H, H^5], 6.68 [d, ^3J(H,H) = 8.2 Hz, 4 H, H^8], 6.65 [d, ^3J(H,H) = 8.2 Hz, 8 H, H^4], 6.61 [d, ^3J(H,H) = 8.2 Hz, 8 H, H^6], 6.45 [d, ^3J(H,H) = 8.1 Hz, 4 H, H^2], 5.80 [d, ^3J(H,H) = 8.1 Hz, 4 H, H^1], 1.13 [s, 36 H, C(CH_3)$_3$], 1.11 [s, 54 H, C(CH_3)$_3$] ppm. $^{13}C\{^1H\}$ NMR (151 MHz, $CDCl_3$, 25 °C): δ = 147.3 (C_{quat}), 147.3 (C_{quat}), 147.2 (C_{quat}), 140.6 (C_{quat}), 140.1 (C_{quat}), 140.1 (C_{quat}), 139.7 (C_{quat}), 138.0 (C_{quat}), 138.0 (C_{quat}), 137.2 (C_{quat}), 135.0 [pt, J(P,C) = 6.6 Hz, 12 C, *C*H, C^o], 131.4 (m, 6 C, C_{quat}, C^i), 131.2 (s, 8 C, *C*H, C^4), 131.1 (s, 4 C, *C*H, C^8), 131.0 (s, 8 C, *C*H, C^6), 130.3 (s, 4 C, *C*H, C^2), 130.0 (s, 12 C, *C*H, C^p), 129.9 (s, 4 C, *C*H, C^1), 127.6 [pt, J(P,C) = 5.5 Hz, 12 C, *C*H, C^m], 124.8 (C_{quat}), 123.0 (s, 8 C, *C*H, C^3), 123.0 (s, 4 C, *C*H, C^7), 122.9 (s, 8 C, *C*H, C^5), 120.7 (C_{quat}), 116.4 (2 C, C_{quat}, C≡C), 114.1 (2 C, C_{quat}, C≡C), 34.1 (4 C, C_{quat}), 34.0 (2 C, C_{quat}), 34.0 (4 C, C_{quat}), 31.3 [s, 12 C, C(*C*H$_3$)$_3$], 31.2 [s, 18 C, C(*C*H$_3$)$_3$] ppm. $^{31}P\{^1H\}$ NMR (162 MHz, $CDCl_3$, 25 °C): δ = 19.31 [^1J(P,Pt) = 2657 Hz, *P*Ph$_3$] ppm. IR: $\tilde{\nu}$ = 2110 cm^{-1} (C≡C) cm^{-1}. MS (MALDI-TOF, $CHCl_3$): calcd. for $[C_{164}H_{168}P_2Pt]^+$ 2394.2269; found 2394.2241 $[M]^+$. $C_{164}H_{168}P_2Pt{\cdot}CH_3OH$ (2428.18): calcd. C 81.62, H 7.14; found C 81.33, H 7.31.

***trans*-[Pt(L²)$_2$(PPh$_3$)$_2$] (T²): T²** was prepared according to the general synthetic procedure by using **L²** (100.3 mg, 0.121 mmol), *cis*-$PtCl_2(PPh_3)_2$ (39.9 mg, 0.060 mmol), and CuI (1.1 mg, 10 mol-%) in still-dried CH_2Cl_2/*i*Pr_2NH (ca. 2.5:1, v/v; 20 mL:8 mL) under argon over 2 d. Column chromatography on silica was performed by eluting first with petroleum ether/chloroform (3:2, v/v) and later with petroleum ether/chloroform (1:2, v/v). Precipitation yielded the product as a deep yellow powder (101.2 mg, 71.0%). M.p. > 360 °C. ^1H NMR (600 MHz, $CDCl_3$, 25 °C): δ = 9.33 (m, 16 H, H^3, H^4, H^5, H^6), 8.95 (s, 4 H, H^2), 8.42 (s, 4 H, H^1), 8.21 (m, 12 H, H^o), 7.54 [t, ^3J(H,H) = 7.5 Hz, 12 H, H^m], 7.46 [t, ^3J(H,H) = 7.5 Hz, 6 H, H^p], 1.86 [s, 54 H, C(CH_3)$_3$], 1.82 [s, 36 H, C(CH_3)$_3$] ppm. $^{13}C\{^1H\}$ NMR (100.6 MHz, $CDCl_3$, 25 °C): δ = 149.0 (C_{quat}), 148.9 (C_{quat}), 135.5 [pt, J(P,C) = 5.9 Hz, 12C, *C*H, C^o], 131.3 [pt, AXX′, ^1J(P,C) + ^3J(P,C) = 29.3 Hz, 6 C, C_{quat}, C^i], 130.7 (s, 6 C, *C*H, C^p), 130.5 (m, C_{quat}), 130.3 (C_{quat}), 130.2 (C_{quat}), 130.0 (C_{quat}), 128.1 [pt, J (P,C) = 4.9 Hz, 12 C, *C*H, C^m], 126.8 (C_{quat}), 124.6 (s, 4 C, *C*H, C^2), 124.1 (C_{quat}), 124.0 (C_{quat}), 123.9 (C_{quat}), 123.6 (C_{quat}), 120.8 (C_{quat}), 120.5 (C_{quat}), 120.4 (C_{quat}), 120.4 (C_{quat}), 119.3 (s, 4 C, *C*H, C^1), 118.9 (s, 12 C, *C*H, C_{HBC}), 118.6 (s, 4 C, *C*H, C_{HBC}), 115.4 (2 C, C_{quat}, C≡C), 113.7 (2 C, C_{quat}, C≡C), 35.8 [4 C, C_{quat}, *C*(CH$_3$)$_3$], 35.8 [6 C, C_{quat}, *C*(CH$_3$)$_3$], 32.1 [s, 12 C, C(*C*H$_3$)$_3$], 32.0 [s, 18 C, C(*C*H$_3$)$_3$] ppm. $^{31}P\{^1H\}$ NMR (162 MHz, $CDCl_3$, 25 °C): δ = 18.96 [^1J(P,Pt) = 2625 Hz, *P*Ph$_3$] ppm. IR: $\tilde{\nu}$ = 2093 (C≡C) cm^{-1}. MS (MALDI-TOF, THF): calcd. for $[C_{164}H_{145}P_2Pt]^+$ 2371.0469; found: 2371.0386 $[M + H]^+$. $C_{164}H_{144}P_2Pt{\cdot}2CH_3OH$ (2436.03): calcd. C 81.85, H 6.29; found C 82.00, H 6.28.

***cis*-[Pt(L¹)$_2$(dppe)] (C¹): C¹** was prepared according to the general synthetic procedure by using **L¹** (100.1 mg, 0.119 mmol), *cis*-$PtCl_2$(dppe) (39.1 mg, 0.059 mmol), and CuI (1.0 mg, 8.9 mol-%) in still-dried CH_2Cl_2/*i*Pr_2NH (ca. 3:1, v/v; 24 mL:8 mL) under argon for 36 h. Following washing, column chromatography on silica was performed by eluting with CH_2Cl_2/hexane (1:1, v/v) as solvent system. Removal of the solvent yielded the product as a pale yellow solid (70.4 mg, 52.6%). M.p. > 235 °C (decomp.). ^1H NMR (600 MHz, $CDCl_3$, 25 °C): δ = 7.90 (m, 8 H, H^o), 7.37 [t, ^3J(H,H) = 7.6 Hz, 4 H, H^p], 7.31 (m, 8 H, H^m), 6.80 (m, 20 H, H_{phenyl}), 6.65 (m, 20 H, H_{phenyl}), 6.63 [d, ^3J(H,H) = 8.3 Hz, 4 H, H^2], 6.58 [d, ^3J(H,H) = 8.3 Hz, 4 H, H^1], 2.38 (m, 4 H, CH_2), 1.12 [m, 90 H, C(CH_3)$_3$] ppm. $^{13}C\{^1H\}$ NMR (151 MHz, $CDCl_3$, 25 °C): δ = 147.3 (C_{quat}), 147.3 (C_{quat}), 147.2 (C_{quat}), 140.5 (C_{quat}), 140.2 (C_{quat}), 140.1 (C_{quat}), 140.0 (C_{quat}), 138.1 (C_{quat}), 138.1 (C_{quat}), 137.8 (C_{quat}), 137.8 (C_{quat}), 133.5 [pt, J(P,C) = 5.5 Hz, 8C, *C*H, C^o], 131.1 (8 C, *C*H), 131.1 (12 C, *C*H), 130.9 (s, 4 C, *C*H, C^p), 130.6 (s, 4 C, *C*H, C^1), 130.1 [pd, ^1J(P,C) = 53.6 Hz, 4C, C_{quat}, C^i], 129.8 (s, 4 C, *C*H, C^2), 128.5 [pt, J(P,C) = 4.9 Hz, 8 C, *C*H, C^m], 124.7 (C_{quat}), 123.1 (8 C, *C*H), 123.0 (4 C, *C*H), 122.9 (8 C, *C*H), 113.0 (2 C, C_{quat}, C≡C), 112.8 (2 C, C_{quat}, C≡C), 34.1 (C_{quat}), 34.0 (C_{quat}), 33.9 (C_{quat}), 31.3 [s, 12 C, C(*C*H$_3$)$_3$], 31.2 [s, 18 C, C(*C*H$_3$)$_3$] 27.8 (s, 2 C, *C*H$_2$) ppm. $^{31}P\{^1H\}$ NMR (162 MHz, $CDCl_3$, 25 °C): δ = 41.26 [^1J(P,Pt) = 2279 Hz, *P*Ph$_2$] ppm. IR: $\tilde{\nu}$ = 2106, 2118 (sh) (C≡C) cm^{-1}. MS (MALDI-TOF, $CHCl_3$): calcd. for $[C_{154}H_{162}P_2Pt]$ 2268.1800; found 2268.1777 $[M]^+$.

$C_{154}H_{162}P_2Pt{\cdot}2H_2O$ (2306.01): C 80.21, H 7.26; found C 80.30, H 7.17.

***cis*-[Pt(L^2)$_2$(dppe)] (C^2):** C^2 was prepared according to the general synthetic procedure by using L^2 (100.1 mg, 0.121 mmol), *cis*-$PtCl_2$(dppe) (40.0 mg, 0.060 mmol), and CuI (0.8 mg, 7 mol-%) in still-dried CH_2Cl_2/*i*Pr_2NH (ca. 3:1, v/v; 24 mL:8 mL) under argon over 2 d. After washing with water (3 × 150 mL), the bright yellow product was precipitated from excess methanol, filtered and washed with cold methanol (3 × 100 mL) (120.8 mg, 89.4%). M.p. > 360 °C. ^{1}H NMR (400.1 MHz, $CDCl_3$, 25 °C): δ = 9.31 (m, 12 H, H_{phenyl}), 9.27 (m, 8 H, H_{phenyl}), 9.22 (s, 4 H, H^1), 8.20 (m, 8 H, H^o), 7.53 (m, 12 H, H^m, H^p), 2.60 (m, 4 H, CH_2), 1.83 [s, 18 H, $C(CH_3)_3$], 1.82 [s, 36 H, $C(CH_3)_3$], 1.78 [s, 36 H, $C(CH_3)_3$] ppm. ^{13}C{^{1}H} NMR (151 MHz, $CDCl_3$, 25 °C): δ = 148.9 (C_{quat}), 148.7 (C_{quat}), 133.6 [pt, *J*(P,C) = 5.5 Hz, 8 C, *C*H, C^o], 131.3 (s, 4 C, C^p), 130.4 (C_{quat}), 130.4 (C_{quat}), 130.3 (C_{quat}), 130.2 (C_{quat}), 130.2 (C_{quat}), 130.1 (C_{quat}), 130.0 [pd, ^1J(P,C) = 55.1 Hz, 4 C, C_{quat}, C^i], 129.6 (C_{quat}), 128.8 [pt, *J*(P,C) = 4.9 Hz, 8 C, *C*H, C^m], 126.4 (C_{quat}), 124.8 (s, *C*H, C_{HBC}), 123.9 (C_{quat}), 123.8 (C_{quat}), 123.7 (C_{quat}), 123.7 (C_{quat}), 120.6 (C_{quat}), 120.4 (C_{quat}), 120.3 (C_{quat}), 120.2 (C_{quat}), 119.5 (s, 4 C, *C*H, C^1), 118.7 (s, *C*H, C_{HBC}), 118.7 (s, *C*H, C_{HBC}), 118.6 (s, *C*H, C_{HBC}), 118.4 (s, *C*H, C_{HBC}), 113.6 (2 C, C_{quat}, C≡C), 112.8 (2 C, C_{quat}, C≡C), 35.6 (C_{quat}), 35.5 (C_{quat}), 31.9 [s, 12 C, $C(CH_3)_3$], 31.8 [s, 18 C, $C(CH_3)_3$], 29.5 (s, 2 C, CH_2) ppm. ^{31}P{^{1}H} NMR (162 MHz, $CDCl_3$, 25 °C): δ = 41.22 [^1J(P,Pt) = 2279 Hz, PPh_2] ppm. IR: $\tilde{\nu}$ = 2109, 2104 (C≡C) cm^{-1}. MS (MALDI-TOF, THF/toluene): calcd. for $[C_{154}H_{139}P_2Pt]^+$ 2245.0000; found 2244.9922 $[M + H]^+$. $C_{154}H_{138}P_2Pt{\cdot}CH_3OH$ (2277.83): C 81.73, H 6.28; found C 81.59, H 6.32.

Supporting Information (see footnote on the first page of this article): Solution UV/Vis spectral data for $L^{1/2}$, $\mathbf{C^{1/2}}$ and $\mathbf{T^{1/2}}$; cyclic voltamogramms of L^2 and C^2 versus Fc/Fc$^+$; normalised emission spectra of L^1, C^1 and T^1 in CH_2Cl_2 glass at 77 K and in the solid state at 298 K; crystal data and structure refinement details for I-HBC.

Acknowledgments

We thank Dr. John O'Brien, Dr. Manuel Ruether, Dr. Martin Feeney, and Dr. Bernard-Jean Denis for technical assistance and Dr. Thomas McCabe and Dr. Longsheng Wang for X-ray crystallography. This material is based upon works supported by the Irish Research Council (Embark) (IRCSET) (PG-Nolan), the European Union Framework 6 Programme (EU FP6) [MKTD-CT-2004-014472] (PD-Gil) and the Science Foundation Ireland [SFIPICA-05] (PD-Murphy).

[1] a) S. Ito, M. Wehmeier, J. D. Brand, C. Kübel, R. Epsch, J. P. Rabe, K. Müllen, *Chem. Eur. J.* **2000**, *6*, 4327–4342; b) J. Wu, W. Pisula, K. Müllen, *Chem. Rev.* **2007**, *107*, 718–747.

[2] a) D. Liu, S. De Feyter, M. Cotlet, A. Stefan, U.-M. Wiesler, A. Herrmann, D. Grebel-Koehler, J. Qu, K. Müllen, F. C. De Schryver, *Macromolecules* **2003**, *36*, 5918–5925; b) D. J. Gregg, C. M. A. Ollagnier, C. M. Fitchett, S. M. Draper, *Chem. Eur. J.* **2006**, *12*, 3043–3052; c) R. E. Bauer, C. G. Clark Jr., K. Müllen, *New J. Chem.* **2007**, *31*, 1275–1282; d) X. Qi, C. Xue, X. Huang, Y. Huang, X. Zhou, H. Li, D. Liu, F. Boey, Q. Yan, W. Huang, S. De Feyter, K. Müllen, H. Zhang, *Adv. Funct. Mater.* **2010**, *20*, 43–49.

[3] a) B. El Hamaoui, F. Laquai, S. Baluschev, J. Wu, K. Muellen, *Synth. Met.* **2006**, *156*, 1182–1186; b) B. El Hamaoui, L. Zhi, J. Wu, J. Li, N. T. Lucas, Z. Tomovic, U. Kolb, K. Mullen, *Adv. Funct. Mater.* **2007**, *17*, 1179–1187; c) K. Y. Kim, S. Liu, M. E. Kose, K. S. Schanze, *Inorg. Chem.* **2006**, *45*, 2509–2519.

[4] a) D. J. Gregg, E. Bothe, P. Hofer, P. Passaniti, S. M. Draper, *Inorg. Chem.***2005**, *44*, 5654–5660; b) D. J. Roberts, D. J. Gregg, C. M. Fitchett, S. M. Draper, *Organometallics* **2010**, *29*, 6541–6547; c) A. Woolf, A. B. Chaplin, J. E. McGrady, M. A. M. Alibadi, N. Rees, S. M. Draper, F. Murphy, A. S. Weller, *Eur. J. Inorg. Chem.* **2011**, *10*, 1614–1625.

[5] a) V. W.-W. Yam, *Acc. Chem. Res.* **2002**, *35*, 555–563; b) J. A. G. Williams, S. Develay, D. L. Rochester, L. Murphy, *Coord. Chem. Rev.* **2008**, *252*, 2596–2611.

[6] a) E. E. Silverman, T. Cardolaccia, X. Zhao, K.-Y. Kim, K. Haskins-Glusac, K. S. Schanze, *Coord. Chem. Rev.* **2005**, *249*, 1491–1500; b) Y. Liu, Y. Li, K. S. Schanze, *J. Photochem. Photobiol. C: Photochem. Rev.* **2002**, *3*, 1–23.

[7] a) J. S. Wilson, A. Köhler, R. H. Friend, M. K. Al¿Suti, M. R. A. Al¿Mandhary, M. S. Khan, P. R. Raithby, *J. Chem. Phys.* **2000**, *113*, 7627–7634; b) J. S. Wilson, N. Chawdhury, M. R. A. Al-Mandhary, M. Younus, M. S. Khan, P. R. Raithby, A. Köhler, R. H. Friend, *J. Am. Chem. Soc.* **2001**, *123*, 9412–9417.

[8] a) J. Fornies, M. A. Gomez-Saso, E. Lalinde, F. Martinez, M. T. Moreno, *Organometallics* **1992**, *11*, 2873–2883; b) R. Saha, M. A. Qaium, D. Debnath, M. Younus, N. Chawdhury, N. Sultana, G. Kociok-Koehn, L.-l. Ooi, P. R. Raithby, M. Kijima, *Dalton Trans.* **2005**, 2760–2765.

[9] K. Haskins-Glusac, I. Ghiviriga, K. A. Abboud, K. S. Schanze, *J. Phys. Chem. B* **2004**, *108*, 4969–4978.

[10] F. A. Murphy, S. M. Draper, *J. Org. Chem.* **2010**, *75*, 1862–1870.

[11] a) Y. Fujikura, K. Sonogashira, N. Hagihara, *Chem. Lett.* **1975**, 1067–1070; b) K. Sonogashira, S. Takahashi, N. Hagihara, *Macromolecules* **1977**, *10*, 879–880; c) K. Sonogashira, T. Yatake, Y. Tohda, S. Takahashi, N. Hagihara, *J. Chem. Soc., Chem. Commun.* **1977**, 291–292.

[12] G. Booth, J. Chatt, *J. Chem. Soc. A* **1966**, 634–638.

[13] J. C. J. Bailar, H. Itatani, *Inorg. Chem.* **1965**, *4*, 1618–1620.

[14] I. B. Berlman, H. O. Wirth, O. J. Steingraber, *J. Phys. Chem.* **1971**, *75*, 318–325.

[15] a) J. Wu, A. Fechtenkotter, J. Gauss, M. D. Watson, M. Kastler, C. Fechtenkotter, M. Wagner, K. Müllen, *J. Am. Chem. Soc.* **2004**, *126*, 11311–11321; b) C. J. Martin, B. Gil, S. D. Perera, S. M. Draper, *Eur. J. Org. Chem.* **2011**, DOI: 10.10021ejoc.2011003322.

[16] A. Diez, J. Fernandez, E. Lalinde, M. T. Moreno, S. Sanchez, *Dalton Trans.* **2008**, 4926–4936.

[17] P. T. Herwig, V. Enkelmann, O. Schmelz, K. Müllen, *Chem. Eur. J.* **2000**, *6*, 1834–1839.

[18] B. El Hamaoui, F. Laquai, S. Baluschev, J. Wu, K. Müllen, *Synth. Met.* **2006**, *156*, 1182–1186.

[19] C. J. Martin, B. Gil, S. M. Draper, *Chem. Commun.* **2011**, *47*, 3616–3618.

[20] P. Four, F. Guibe, *J. Org. Chem.* **1981**, *46*, 4439–4445.

[21] G. A. Crosby, J. N. Demas, *J. Phys. Chem.* **1971**, *75*, 991–1024.

[22] D. F. Eaton, *Pure Appl. Chem.* **1988**, *60*, 1107–1114.

[23] T. Hard, P. Fan, D. R. Kearns, *Photochem. Photobiol.* **1990**, *51*, 77–86.

Received: April 19, 2011
Published Online: June 21, 2011

